Supporting information

The influence of the tethered dopants templates on the electrochemical, nanomorphological, and nanomechanical properties of 2D conductive polymer film

Luiza A. Nascimento[a,b,c], Kilian S. Fraysse[d], Daniel P. Langley[a,b,c], Rosanne M. Guijt[e], Paul R. Stoddart[f], Simon Moulton[f,g,h,i], Saimon Moraes Silva[a,b,c], George W. Greene[a,b,c].*

[a.] The Biomedical and Environmental Sensor Technology (BEST) Research Centre, La Trobe Institute for Molecular Science (LIMS), La Trobe University, Melbourne, Victoria 3086, Australia.

[b.] Department of Biochemistry and Chemistry, School of Agriculture, Biomedicine and Environment (SABE), La Trobe University, Melbourne, Victoria 3086, Australia.

[c.] ARC Research Hub for Molecular Biosensors at Point-of-Use (MOBIUS), La Trobe University, Melbourne, Victoria 3086, Australia

[d.] Centre for Regional and Rural Futures, Deakin University, Geelong, Victoria 3220, Australia

[e.] Centre for Regional and Rural Futures, Deakin University, Geelong, Victoria 3220, Australia

[f.] School of Engineering, Swinburne University of Technology, Melbourne, VIC 3122, Australia

[g.] The Aikenhead Centre for Medical Discovery, St Vincent's Hospital Melbourne, Melbourne, VIC 3065, Australia

[h.] Iverson Health Innovation Research Institute, Swinburne University of Technology, Melbourne, VIC 3122, Australia

[i.] Department of Advanced Components and Materials Engineering, Sunchon National University, 255, Jungang-ro, Suncheon-si, Jellanam-do 57922, Republic of Korea

[*] w.greene@latrobe.edu.au

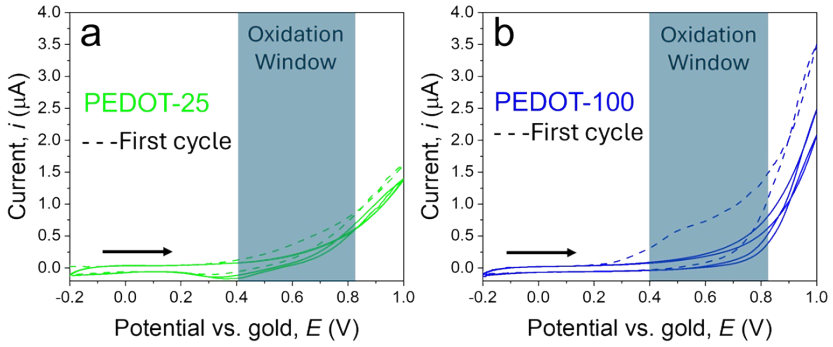

Figure S1: Cyclic voltammograms for the electropolymerization of PEDOT using a) ss-poly(dT)$_{25}$ and b) ss-poly(dT)$_{100}$. Dashed line is the first CV cycle, solid lines represent further cycles. Black arrows indicate direction of sweep.

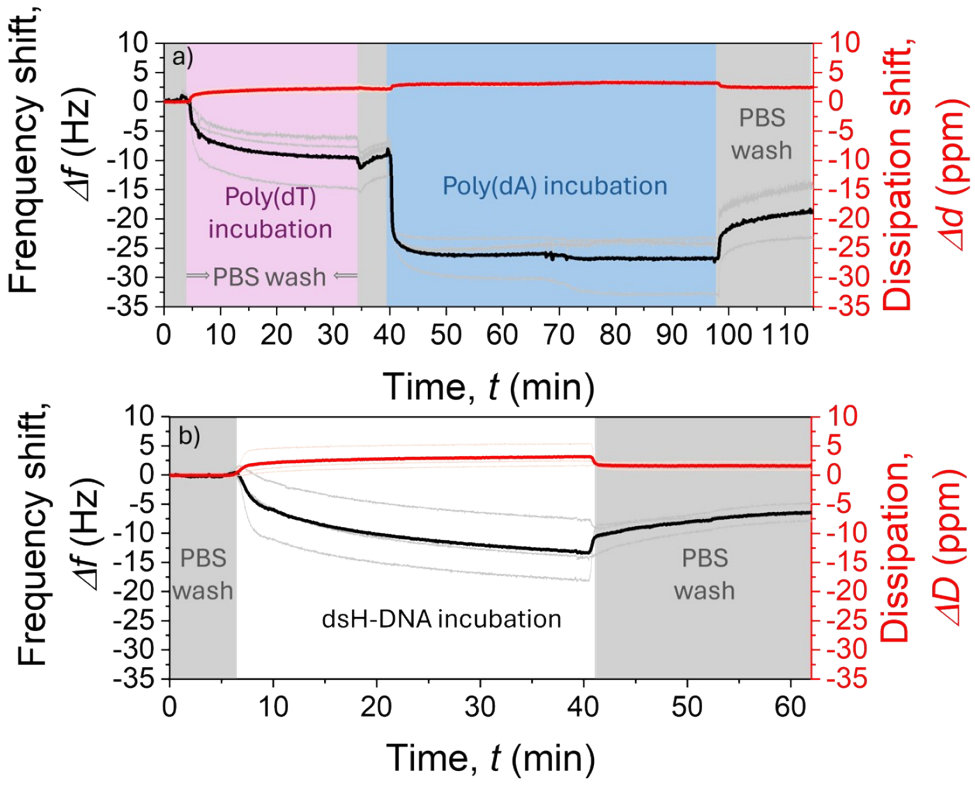

Figure S2: a) Frequency and dissipation measured in-situ for the grafting of thiolated poly(dT) ssDNA followed by hybridization on the surface with poly(dA) ssDNA and b) frequency and dissipation measured in-situ for the grafting of dsDNA hybridized in solution (dsH-DNA). Grey curves are measured frequency shift and black curve is the averaged of the three measured frequency shift. As for the frequency, the light pink curves are the measured dissipation shift, and the red curve is the averaged of the dissipation shift.

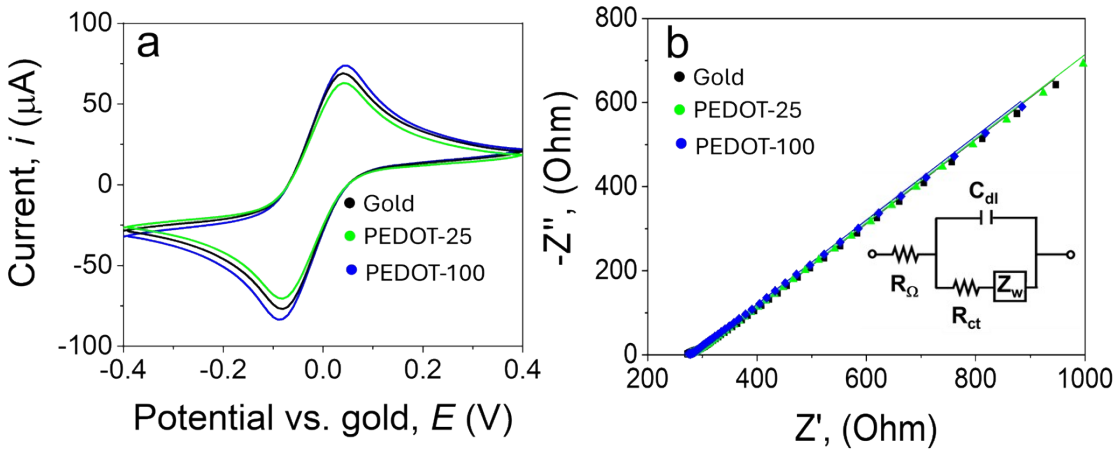

Figure S3: Cyclic voltammograms for 2D PEDOT doped with different DNA layers in a) 3.6 mM ferri/ferro in 1.0 M KCl at 50mV/s in a potential window of -0.4V to +0.4V. b) EIS in ferri/ferro solution for 2D PEDOT doped with different DNA layers at 0.0V from $1x10^6$ Hz to 0.1 Hz.

Table S1: Values of R_{ct} and C_{dl} for gold and 2D PEDOT films doped with tethered ssDNA of different chain lengths simulated through Randles circuit from EIS data.

Surface	**PEDOT-25**	**PEDOT-100**
Rct (ohm)	8.9±0.6	4.6±0.8
Cdl (μF)	3.3±0.4	1.6±0.5

Table S2: Statistical values on the different 2D PEDOT surfaces calculated from the AFM images.

Surfaces	**PEDOT-25**	**PEDOT-100**
RMS roughness (nm)	4.5	2.9
peak-valley roughness (nm)	14.9	6.5

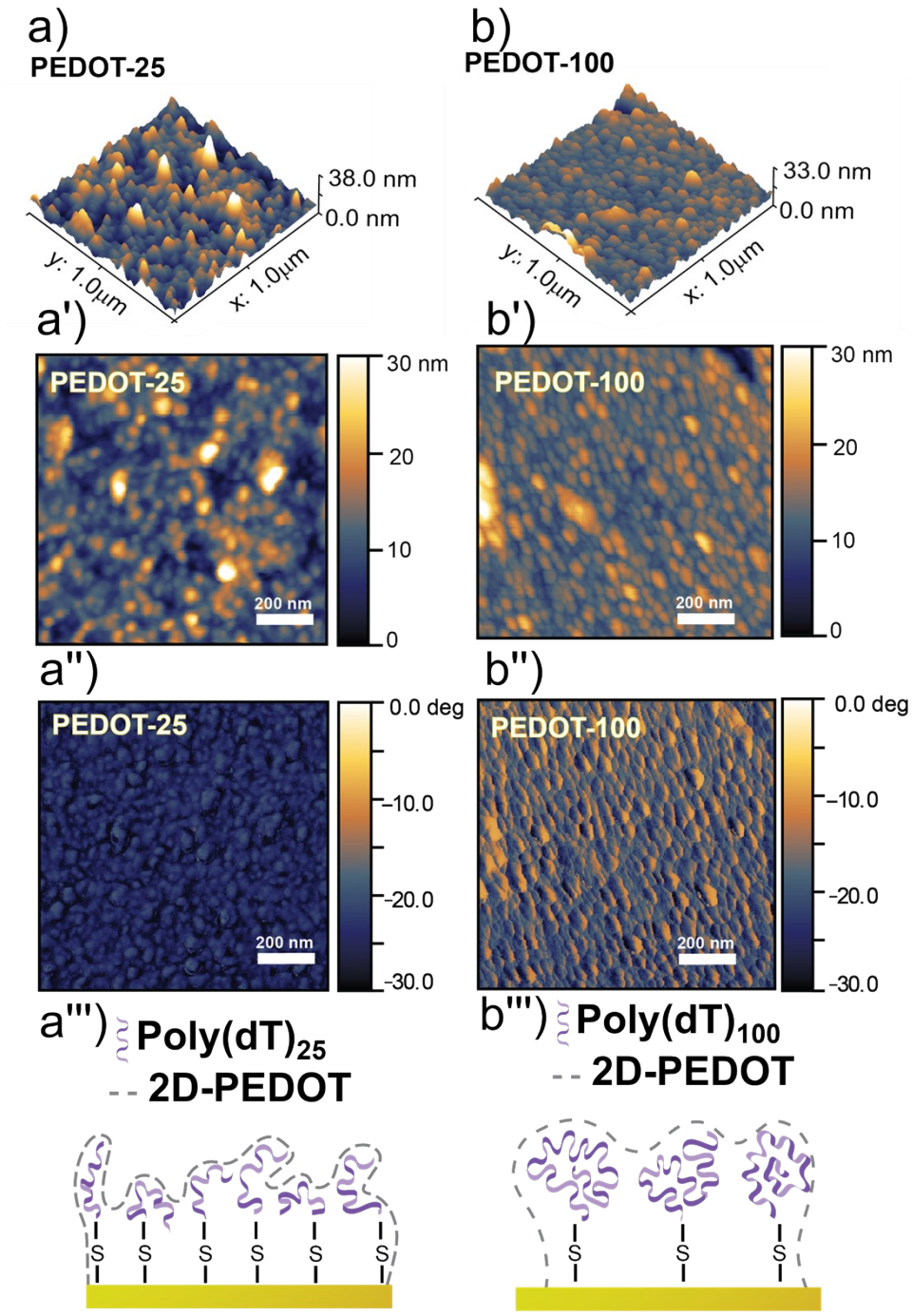

Figure S3: 3D representation of the AFM topography scan for a) PEDOT-25 and b) PEDOT-100 rotated at φ = 45 and θ = -45. 3D representation of the AFM topography scan for a') PEDOT-25 and b') PEDOT-100 respective phase images a'' and b''. Graphic representation of end-grafted ssDNA layer conformation for a''') ss-poly(dT)$_{25}$ b''') ss-poly(dT)$_{100}$

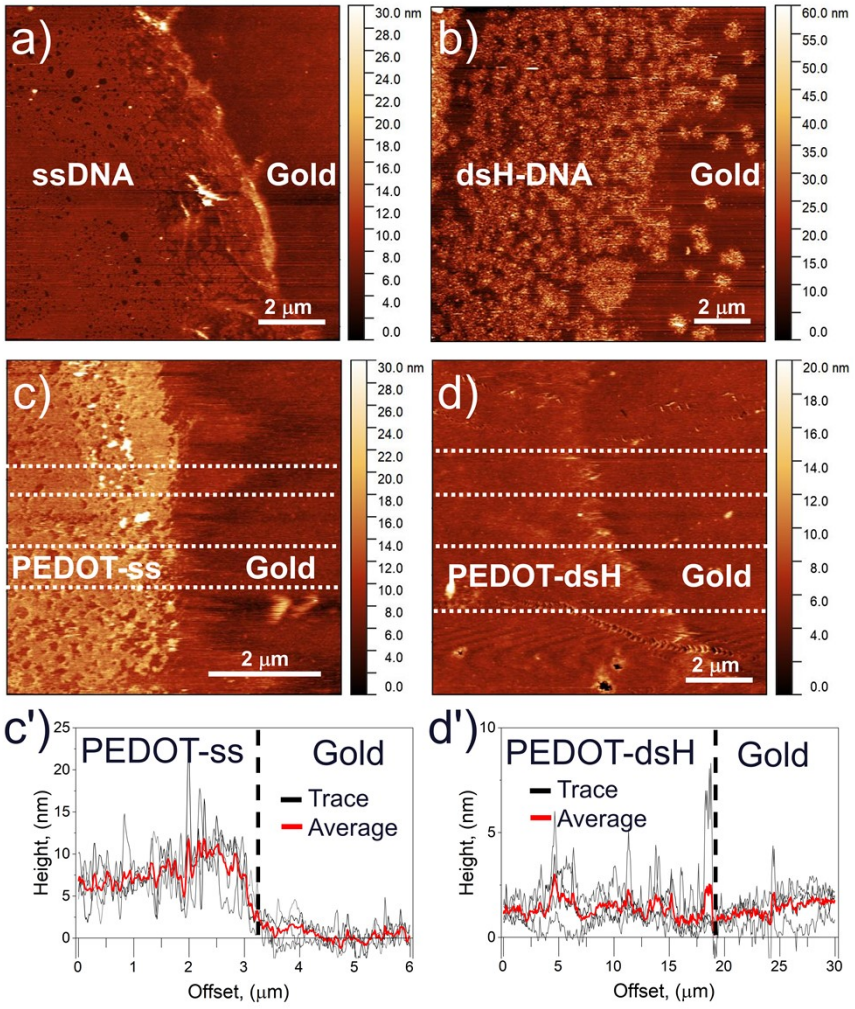

Figure S4: AFM topography images for the edge of a) ssDNA, b) dsH-DNA, c) PEDOT-ss and d) PEDPT-dsH. Height traces for c') PEDOT-ss and d') PEDOT-dsH. Grey lines correspond to the white dashed lines in c) and d) and red is the average trace. Note that figure resolution and color scale are individually adjusted to show surface features.